Synthesis, Molecular Modeling, and Opioid Receptor Affinity of 9,10-Diazatricyclo[4.2.1.1^{2,5}]decanes and 2,7-Diazatricyclo[4.4.0.0^{3,8}]decanes Structurally Related to 3,8-Diazabicyclo[3.2.1]octanes

Paola Vianello,[▽,§] Alberto Albinati,[§] Gerardo A. Pinna,[∥] Antonio Lavecchia,[†] Luciana Marinelli,[†] Pier Andrea Borea,[‡] Stefania Gessi,[‡] Paola Fadda,[⊥] Silvia Tronci,[⊥] and Giorgio Cignarella*[,§]

Istituto di Chimica Farmaceutica e Tossicologica, Viale Abruzzi 42, 20131 Milano, Italy, Dipartimento Farmaco Chimico Tossicologico, Via Muroni 23/A, 07100 Sassari, Italy, Dipartimento di Chimica Farmaceutica e Tossicologica, Università di Napoli "Federico II", Via D. Montesano 49, 80131 Napoli, Italy, Dipartimento di Medicina Clinica e Sperimentale, Via Fossato di Mortara 19, 44100 Ferrara, Italy, and Dipartimento di Neuroscienze, Via Porcell 4, 09100 Cagliari, Italy

Received August 2, 1999

Various lines of evidence, including molecular modeling studies, imply that the endoethylenic bridge of 3,8-diazabicyclo[3.2.1]octanes (DBO, **1**) plays an essential role in modulating affinity toward μ opioid receptors. This hypothesis, together with the remarkable analgesic properties observed for N_3 propionyl, N_8 arylpropenyl derivatives (**2**) and of the reverted isomers (**3**), has prompted us to insert an additional endoethylenic bridge on the piperazine moiety in order to identify derivatives with increased potency toward this receptor class. In the present report, we describe the synthesis of the novel compounds 9,10-diazatricyclo[4.2.1.1^{2,5}]decane (**4**) and 2,7-diazatricyclo[4.4.0.0^{3,8}]decane (**5**), as well as the representative derivatives functionalized at the two nitrogen atoms by propionyl and arylpropenyl groups (**6a**−**e**, **7a**−**d**). Opioid receptor binding assays revealed that, among the compounds tested, the N-propionyl-N-cinnamyl derivatives **6a** and **7a** exhibited the highest μ-receptor affinity, and remarkably, compound **7a** displayed in vivo (mice) an analgesic potency 6-fold that of morphine.

Introduction

The nucleus of 3,8-diazabicyclo[3.2.1]octane (see Chart 1, DBO, **1**),[1] when substituted on the N_3 and N_8 by propionyl and by an arylalkenyl group (**2**, **3**), has yielded compounds endowed with a central analgesic activity comparable to, or higher than, that of morphine.[2] More recently it was found that the analgesic activity of DBOs is related to their interaction with opioid μ-receptors with affinity in the nanomolar range, similarly to morphine, but with a higher μ/δ selectivity.[3,4]

The μ-receptor affinity and analgesic potency of these compounds, as compared with the loss of activity for the corresponding piperazine and equatorial 2,6-dimethylpiperazine derivatives, suggested that the endoethylenic bridge of DBO plays an essential role in interacting with the receptor, possibly by fitting into a lipophilic pocket.[5] Indeed, the finding that the μ-affinity of certain 3-arylpropenyl-8-propionyl-DBO derivatives is retained or even improved by reverting the position of the 3,8 substituents suggests that the receptor ligand binding site may in fact possess two such pockets, able to accommodate the endoethylenic bridges of the two series.[5]

On the basis of this assumption, we reasoned that a structure bearing two bridges on the piperazine moiety would more efficiently interact with the μ-receptor. Two structures with this requisite are 9,10-diazatricyclo-[4.2.1.1^{2,5}]decane **4**, which has the endoethylenic bridges bonded to carbon atoms 1.6 and 2.5, and 2,7-diazatricyclo-[4.4.0.0^{3,8}]decane **5**, which has the bridges bonded to carbon atoms 1−8 and 3−6 (see Chart 2). Both compounds are so far undescribed in the literature.

An appropriate substitution of the nitrogen atoms of **4** and **5** with a propionyl and an arylpropenyl group

Chart 1

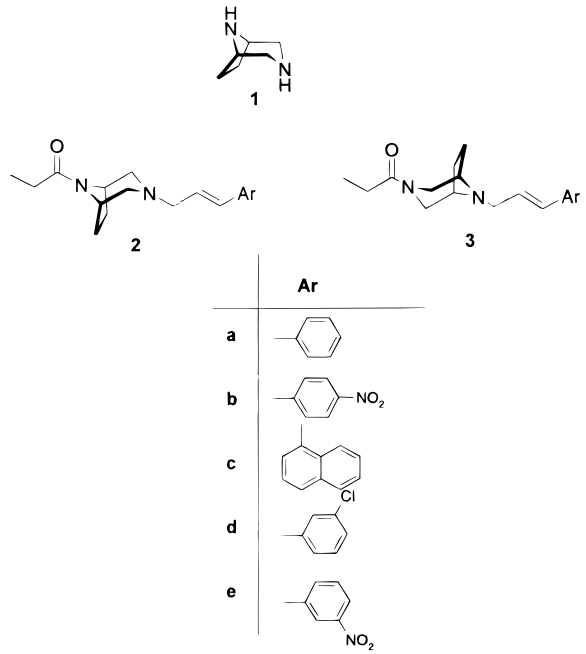

* To whom correspondence should be addressed. Tel: 39-2-29510843. Fax: 39-2-29514197. E-mail: giorgio.cignarella@unimi.it.
§ Istituto di Chimica Farmaceutica e Tossicologica.
∥ Dipartimento Farmaco Chimico Tossicologico.
† Università di Napoli "Federico II".
‡ Dipartimento di Medicina Clinica e Sperimentale.
⊥ Dipartimento di Neuroscienze.
▽ Current address: Pharmacia & Upjohn, V.le Pasteur 10, 20014 Nerviano (MI), Italy.

10.1021/jm991140q CCC: $19.00
Published on Web 05/12/2000

Chart 2

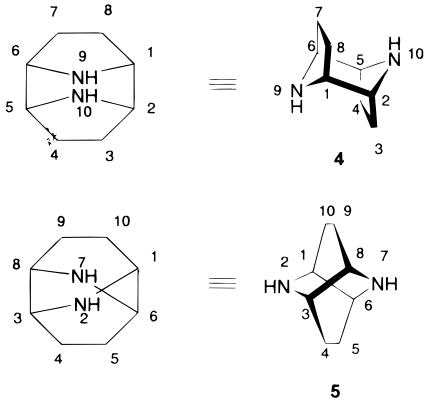

4

5

Chart 3

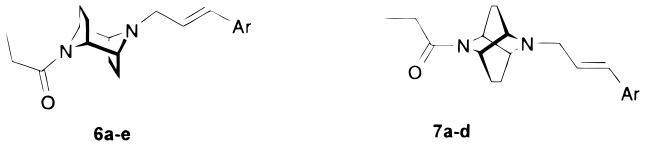

6a-e **7a-d**

a: Ar= C_6H_5
b: p-NO_2-C_6H_5
c: m-NO_2-C_6H_5
d: m-Cl-C_6H_5
e: 1-naphtyl

Scheme 1[a]

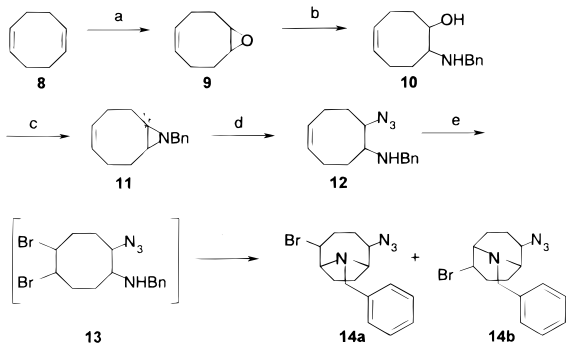

[a] (a) CH_3COOOH; (b) $BnNH_2$, $Yb(OTf)_3$, CH_2Cl_2, rt; (c) (1) $ClSO_3H$, Et_2O, 0−5 °C, (2) NaOH, reflux; (d) NaN_3, NH_4Cl, EtOH/H_2O; (e) Br_2, cyclohexane, 0−5 °C.

would give compounds **6** and **7** (see Chart 3), related to the analgesic DBOs, suitable for verifying our hypothesis.

In this paper, we describe the synthesis of **4** and **5**, and the binding activity to μ-, δ-, and κ-receptors of the related derivatives (**6a**−**e**, **7a**−**d**). Representative terms **6a** and **7a** were also evaluated for their in vivo activity.

Chemistry

The synthesis of **4** and **5** involves *trans*-8-azido-*N*-benzyl-4-cycloocten-1-amine **12** as the common intermediate, easily obtained from the commercially available 1,5-cyclooctadiene (**8**). As outlined in Scheme 1, reaction of **8** with peracetic acid led to the known 9-oxabicyclo[6.1.0]non-4-ene[6] (**9**), which by addition of benzylamine in the presence of ytterbium(III) trifluoromethansulfonate[7] led to 83% of *trans*-8-benzylamino-4-cycloocten-1-ol (**10**). Cyclization of **10** as the sulfate ester in refluxing sodium hydroxide gave 9-benzyl-9-azabicylo[6.1.0]non-4-ene (**11**), which by reaction with sodium azide in refluxing aqueous ethanol led to 91% *trans*-8-azido-*N*-benzyl-4-cycloocten-1-amine **12** as an oil purified by silica gel flash chromatography. Bromination of **12** in cyclohexane at 5 °C led to a not isolated dibromoderivative (**13**), which evolved to a mixture of two isomers separated by silica gel flash chromatography and identified as 2-azido-9-benzyl-5-bromo-9-azabicyclo[4.2.1]nonane (**14a**) (23% yield) and 2-azido-9-benzyl-6-bromo-9-azabicyclo[3.3.1]nonane (**14b**) (19% yield). The assignment of the structures to **14b** and indirectly to **14a** was based on X-ray diffraction analysis of crystals of **14b** (see Figure 1).

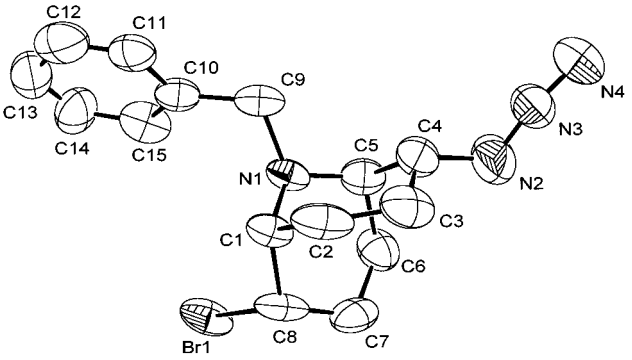

Figure 1. ORTEP view of compound **14b**. Elipsoids drawn at 50% probability.

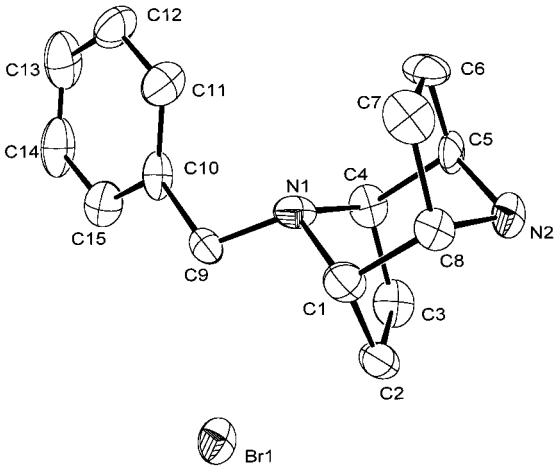

Figure 2. ORTEP view of compound **15**.

Scheme 2[a]

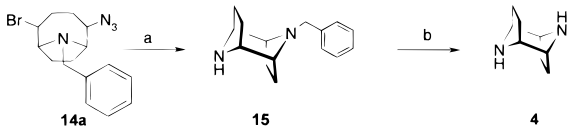

[a] (a) (1) PPh_3, THF, reflux, (2) H_2O, reflux; (b) H_2, Pd/C, EtOH.

The final conversion of **14a** to **4** is reported in Scheme 2. Reduction of the azido group of **14a** with triphenylphosphine in refluxing THF, followed by addition of water at reflux, involved a concomitant cyclization to 85% of 9-benzyl-9,10-diazatricyclo[4.2.1.$1^{2,5}$]decane **15** isolated as the mono hydrobromide whose structure was supported by X-ray diffraction analysis of crystals (see Figure 2).

Debenzylation of **15** by catalytic hydrogenation (Pd/C) in acidic (HCl) ethanol led to 9,10-diazatricyclo-[4.2.1.$1^{2,5}$]decane (**4**) isolated as the dihydrochloride in almost quantitative yield.

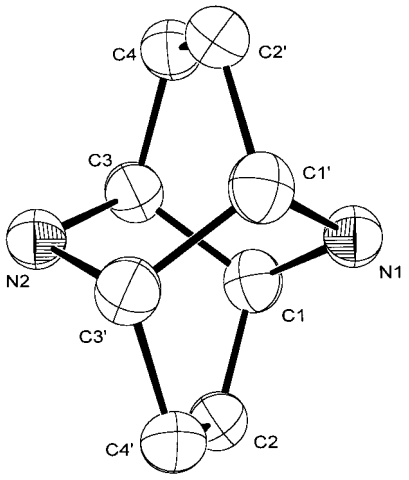

Figure 3. ORTEP view of compound **5**. Primed atoms are related to those unprimed by the symmetry operation: 0.5 − *x*; 1.5 − *y*; *z*.

Scheme 3[a]

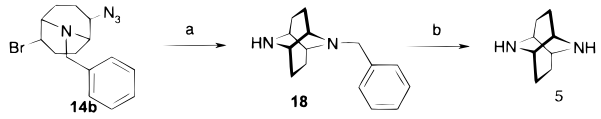

[a] (a) (1) PPh_3, THF, reflux, (2) H_2O, reflux; (b) H_2, Pd/C, EtOH.

Similarly the isomer 2,7-diazatricyclo[4.4.0.0^{3,8}]decane **5** was obtained from **14b** by reductive cyclization to the 9-benzyl derivative **18** followed by debenzylation (Scheme 3). The structure of **5** was supported by X-ray diffraction analysis (see Figure 3).

The availability of the key intermediates **15** and **18** allowed the synthesis of the *N*-aralkenyl-*N*′-propionyl-diazatricyclodecanes **6a**−**e** and **7a**−**d** analogues of the analgesic DBOs, as depicted in Scheme 4. A standard procedure involving propionylation to *N*-benzyl-*N*′-propionyl derivatives **16** and **19**, debenzylation (H_2/Pd) to **17** and **20**, and final alkylation with the appropriate arylalkenyl chloride and K_2CO_3 in refluxing acetone to **6a**−**e** and **7a**−**d** was followed.

Results and Discussion

The new compounds were submitted to binding studies on opioid receptors on mouse brain homogenates in the presence of ^{3}H-DAMGO for μ and ^{3}H-DELTORPHINE II for δ; ^{3}H-U69593 was used on guinea pig homogenates to evaluate κ-binding, using morphine as the reference compound (see Table 1).

Among the compounds tested, the *N*-propionyl-*N*-cinnamyl derivatives **6a** and **7a** exhibited the highest μ-affinity, with K_i's of 10 nM and 7 nM, respectively, which compare favorably to that of the parent DBO (K_i 50 and 160 nM for **2a** and **3a**, respectively). On the contrary, the μ-affinity of the other derivatives was lower by 1 or 2 orders of magnitude than that of the corresponding DBO. These data suggest that the substituent of the aromatic moiety of the side chain in **6** and **7** plays a different role with respect to the parent DBO in eliciting affinity toward μ-receptor.

The two lead compounds, **6a** and **7a**, displaying the highest μ-affinity were evaluated for their analgesic activity by the hot plate test in mice. As shown in Figure 4, **6a** produces a dose-related increase in response latency with an ED_{50} of 9.76 mg/kg ip, thus indicating an analgesic potency lower than that reported[3] for the parent DBO **2a** (ED_{50} = 1.1 mg/kg ip) but higher than that of the reverse isomer **3a** (ED_{50} = 16 mg/kg ip).

Scheme 4[a]

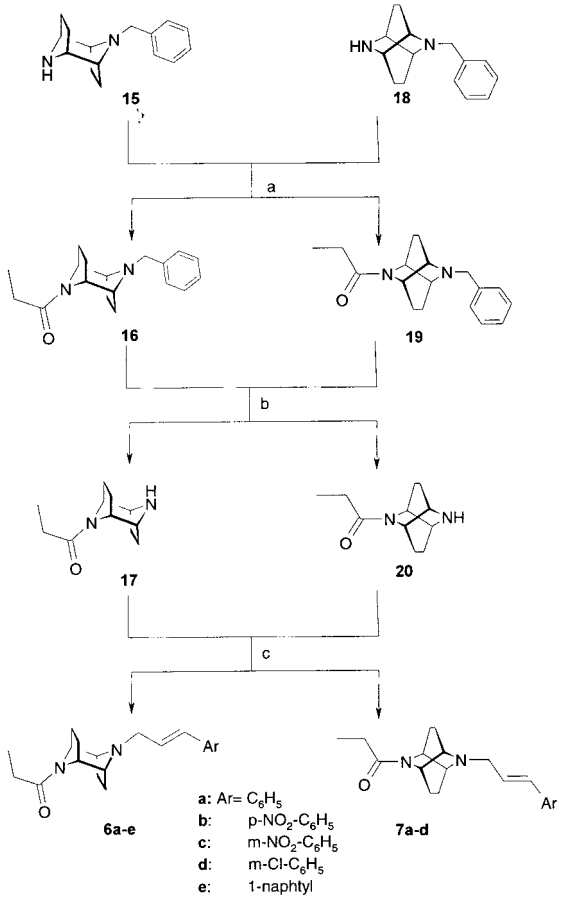

[a] (a) $(CH_3CH_2CO)_2O$, CH_2Cl_2, reflux; (b) H_2, Pd/C, EtOH; (c) $ArCH{=}CHCH_2Cl$, K_2CO_3, acetone, reflux.

Interestingly a definitely higher analgesic potency is displayed by compound **7a** (Figure 5) with an ED_{50} of 0.84 mg/kg ip. Since in the same experimental conditions the ED_{50} for morphine was 5 mg/kg, the analgesic activity of **7a** appears to be 6-fold that of the reference compound. Furthermore, as shown in Figures 6 and 7, the antinociceptive activity of compounds **6a** and **7a** is completely abolished if mice are previously treated with the opioid antagonist naloxone at the dose of 1 mg/kg ip, thus demonstrating an antinociception induced specifically mediated by the opioid receptor.

Molecular Modeling. Molecular modeling studies were carried out in order to rationalize the high affinity of diazatricyclodecane compounds **6a** and **7a** at μ-opioid receptors. We wished to explore their binding mode by building a three-dimensional model of the complex formed between these compounds and the receptor.

Our study benefited from a rhodopsin-based molecular model for the μ opioid receptor recently reported by Pogozheva et al.[8] In this model, the seven α-helical domains and the extracellular loops (EL) were calculated using the distance geometry algorithm, with hydrogen bonding constraints based on the previously developed general model of the transmembrane α-bundle for rhodopsin-like G-protein coupled receptors.[9]

Table 1. Affinity toward Opioid Receptors K_i (nM)

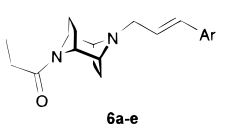

6a-e

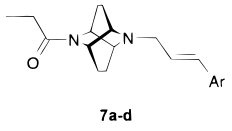

7a-d

compd	Ar	μ	δ	κ	DBO (**2**) μ	DBO (**3**) μ
6a	C_6H_5	10 ± 2	2267 ± 145	3000 ± 145	50	160
6b	*p*-NO_2-C_6H_4-	23 ± 0.6	>10000	>10000	25	5.1
6c	*m*-NO_2-C_6H_4-	40 ± 2.9	7500 ± 289	750 ± 70	10	9.5
6d	*m*-Cl-C_6H_4-	36.6 ± 2			16.33	1.3
6e	1-naphthyl	180 ± 117			21.66	4.66
7a	C_6H_5	7 ± 0.6	500 ± 29	800 ± 40	50	160
7b	*p*-NO_2-C_6H_4-	475 ± 14			25	5.1
7c	*m*-NO_2-C_6H_4-	20 ± 1.2	2233 ± 145	1100 ± 90	10	9.5
7d	*m*-Cl-C_6H_4-	13 ± 0.6	900 ± 58	1200 ± 73	16.33	1.3
morphine		2.8				

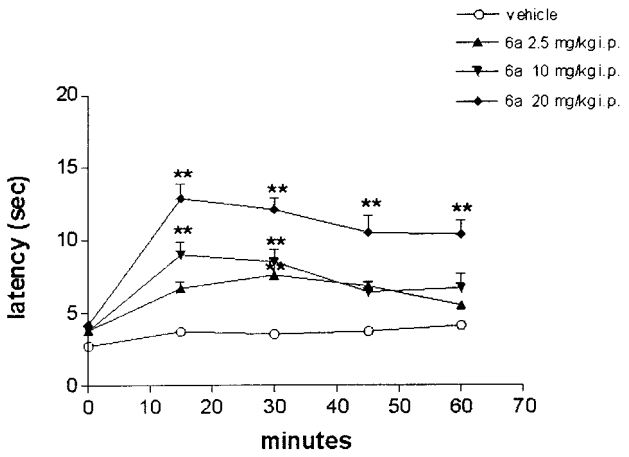

Figure 4. Dose−response curve and time course of **6a** in the hot plate test. Mice received **6a** at the indicated dose at time 0 and were tested on the hot plate every 15 min. Each point represents the mean ± SEM of at least eight mice per group.

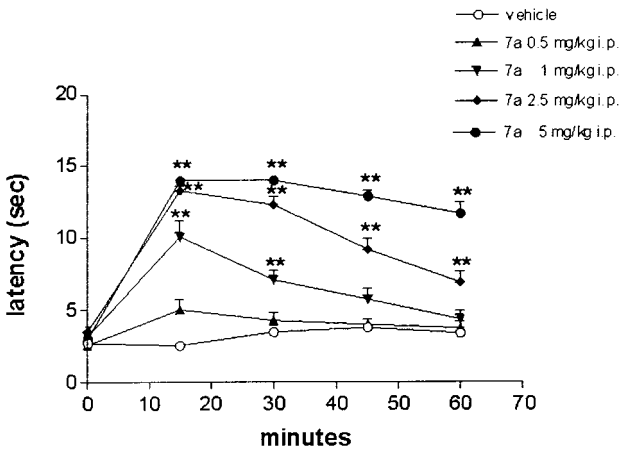

Figure 5. Dose−response curve and time course of **7a** in the hot plate test. Mice received **7a** at the indicated dose at time 0 and were tested on the hot plate every 15 min. Each point represents the mean ± SEM of at least eight mice per group.

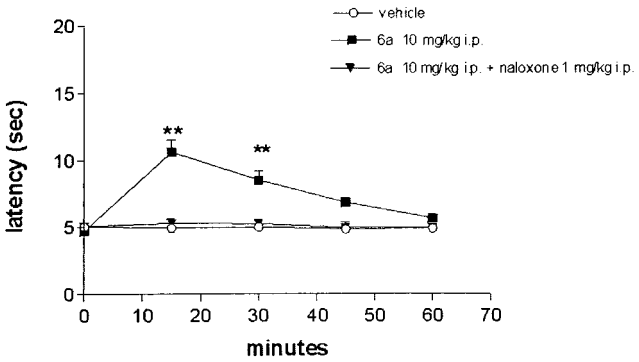

Figure 6. Antagonistic effect of naloxone on **6a**-induced antinociception. Compouond **6a** (10 mg/kg), naloxone (1 mg/kg), or vehicle were administered ip at time 0. Mice were tested on the hot plate every 15 min. Each point represents the mean ± SEM of at least eight mice per group.

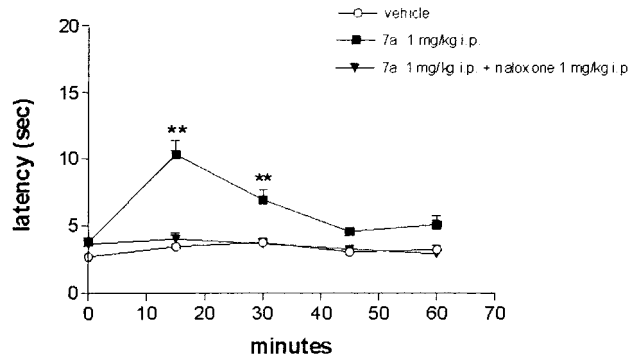

Figure 7. Antagonistic effect of naloxone on **7a**-induced antinociception. Compound **7a** (1 mg/kg), naloxone (1 mg/kg), or vehicle were administered ip at time 0. Mice were tested on the hot plate every 15 min. Each point represents the mean ± SEM of at least eight mice per group.

The computational work was carried out by molecular mechanics, conformational analysis, docking, and graphics routines available within the SYBYL program.[10] Details of these procedures are described in Experimental Section, whereas the results are summarized below.

Both enantiomers of **6a** (2*R*,3*R*,5*S*,6*S* and 2*S*,3*S*,5*R*,6*R*) and **7a** (2*R*,3*R*,5*R*,6*R* and 2*S*,3*S*,5*S*,6*S*) had to be modeled because all the examined compounds were assayed as racemic mixture. Figure 8 shows the enantiomers docked into the putative binding pocket of μ-opioid receptor, after extensive energy minimization and MD simulation cycles. Table 2 collects the amino acids in each TM helix within 5 Å from any atom of the ligand.

Since the degree of stereoelectronic complementarity between the docked enantiomers and the receptor, estimated by the interaction energies, was rather similar, we predict that the enantiomers of each ligand do not exhibit significant differences in potency.

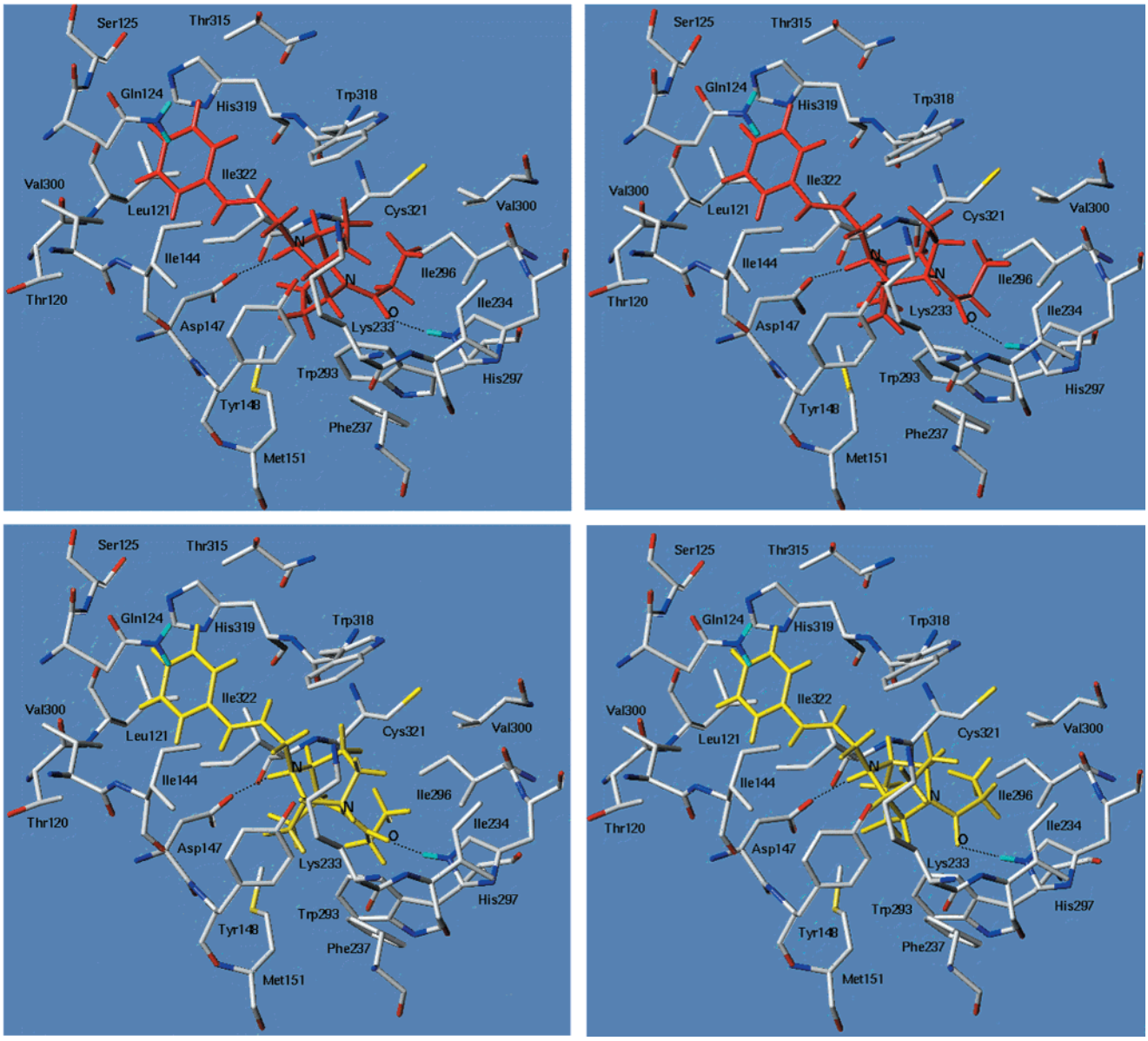

Figure 8. 2*R*,3*R*,5*S*,6*S*-**6a** (top left), 2*S*,3*S*,5*R*,6*R*-**6a** (top right), 2*S*,3*S*,5*S*,6*S*-**7a** (bottom left), and 2*R*,3*R*,5*R*,6*R*-**7a** (bottom right) enantiomers docked into the putative binding pocket of μ-opioid receptor. Only amino acids located within 5 Å distance from any atom at the bound ligand are displayed and labeled. The hydrogen bonds discussed in the text are depicted as black dashed lines.

Table 2. Residues of the μ-Opioid Receptor Binding Site Located within 5 Å from Any Atom of the Docked Enantiomers of **6a** and **7a**[a]

TMII	Thr120; Leu121; Pro122; Gly124; Ser125
TMIII	Val143; Ile144; Asp147; Tyr148; Met151
TMV	Asn230; Lys233; Ile234; Phe237
TMVI	Trp293; Ile296; His297; Val300
TMVII	Trp318; His319; Cys321; Ile322; Gly325
ELIII	Thr315; Ser317

[a] μ-Receptor specific residues are underlined.

The following features of the models are worthy to be outlined. The protonated nitrogen of both **6a**- and **7a**-enantiomers interacts with Asp147 carboxylate group in TMIII through a reinforced ionic bond, as suggested from site-directed mutagenesis data.[11,12] This complex is surrounded by the aromatic residues Tyr148 (TMIII) and Trp318 (TMVII). Such a surrounding of the ammonium−aspartate interaction has also been observed in other models for GPCR−ligand complexes.[13,14] Recently, Verdonk *et al.*[15] showed that in crystal structures R-N$(CH_3)_3^+$ complexes have a specific spatial preference for close contacts with aromatic residues and postulated that such contacts may play a role in ligand−receptor recognition and activation. A hydrogen bond is donated by the His297 imidazole ring to the carbonyl oxygen of the acyl chain of either **6a**- and **7a**-enantiomers (δN−H···O=C distance 1.9 Å). The role of this histidine as hydrogen bond donor seems to be confirmed by the complete loss of affinity of μ-agonist ligands toward the His297/Ala mutant.[11,16] From inspection of the model, it results also that the propionyl chain of **6a** and **7a** is accommodated into a rather large hydrophobic cavity, made up of side chains Ile234 (TMV), Phe237 (TMV), Ile296 (TMVI), Trp293 (TMVI), Val300 (TMVI), Cys321 (TMVII). This is consistent with SAR data indicating that the elongation of the acyl substituent up to a four-carbon atom chain impacts favorably on the binding affinity of diazabicyclooctane derivatives.[17] The two endoethylenic bridges of **6a**- and **7a**-enantiomers contact

Trp293, Trp318, and Met151 (TMIII) side chains, allowing for effective hydrophobic interactions. The importance of Trp318 for the binding of μ-selective ligands has been underscored by site-directed mutagenesis experiments.[18] The styrene moiety fits a hydrophobic pocket of restricted size, delimited by Leu121 (TMII), Val143 (TMIII), Ile322 (TMVII), Thr315 (ELIII), His319 (TMVII), and Gln124 (TMII) side chains. The imidazole ring of His319 is in close proximity to and perpendicularly oriented to the phenyl ring of **6a**- and **7a**-enantiomers, indicating an aromatic−aromatic-type interaction.[19] The planes of the two rings are essentially perpendicular and separated by a distance of 4.7 Å. As suggested by recent site-directed mutagenesis studies, His319 has been proposed as a key residue contributing to the binding of μ-selective agonists.[18]

Experimental Section

Chemistry. Melting points were determined on a Büchi 510 capillary melting point apparatus and are uncorrected. ^{1}H NMR spectra were recorded on a Bruker AC200 spectrometer; chemical shifts are reported as δ (ppm) relative to tetramethylsilane. TLC on silica gel plates was used to check product purity. Flash column chromatography was performed with indicated solvents on silica gel 60 (Merck; 230−240 mesh).

***trans*-8-Benzylamino-4-cycloocten-1-ol (10).** To a stirred solution of 9-oxabicyclo[6.1.0]non-4-ene **9** (10.0 g, 0.081 mol) in dry CH_2Cl_2 (100 mL) kept under nitrogen atmosphere were added benzylamine (10.35 g, 0.097 mol) and ytterbium (III) trifluoromethanesulfonate (4.96 g, 0.008 mol), and the mixture was stirred for 24 h at room temperature. Extractive workup (water, CH_2Cl_2) gave **10** as a white solid (15.46 g, yield 83%): mp = 70−71 °C, bp = 140 °C/1 mm Hg.

^{1}H NMR ($CDCl_3$): δ 1.42−1.95 (m, 2H); 2.02−2.35 (m, 6H); 3.00−3.15 (m, 1H); 3.65−3.75 (m, 1H); 4.07 (AB syst, 2H, J = 12.57 Hz); 5.00−5.42 (bs, D_2O exchangeable); 5.44−5.64 (m, 2H); 7.35−7.38 (m, 3H); 7.56−7.59 (m, 2H).

9-Benzyl-9-azabicyclo[6.1.0]non-4-ene (11). To a suspension of **10** (2.6 g, 0.011 mol) in anhydrous diethyl ether (50 mL) kept at 0−5 °C under vigorous stirring was added chlorosulfonic acid (1.6 g, 0.011 mol) dropwise. The gummy reaction mixture, after additional stirring overnight at room temperature, separated a white solid which was filtered and washed with ether, to give the sulfate ester (3.2 g, yield 93%), mp = 162−163 °C.

^{1}H NMR ($CDCl_3$): δ 1.70−2.60 (m, 8H); 3.30−3.50 (m, 1H); 4.00−4.40 (m, 2H); 4.50−4.70 (m, 1H); 5.30−5.50 (m, 1H); 5.50−5.70 (m, 1H); 7.30−7.50 (m, 5H) 8.00−8.50 (bs D_2O exchangeable, 1H).

The sulfate ester (4 g, 0.017 mol) was added to 33% sodium hydroxide (40 mL), and the resulting solution was refluxed for 2 h, cooled, saturated with potassium hydroxide, and extracted with 3 × 50 mL of ethyl acetate. The organic layers were collected and dried (Na_2SO_4), and the solvent evaporated to give the desired **11** isolated by silica gel flash chromatography eluting with CH_2Cl_2/ethyl acetate 9:1 as an oil: bp = 125 °C/1 mmHg, (2.3 g, yield 62%).

^{1}H NMR ($CDCl_3$): δ 1.45−1.61 (m, 2H); 1.90−2.20 (bm, 6H); 2.25−2.50 (m, 2H); 3.55 (s, 2H); 5.44−5.65 (m, 2H); 7.15−7.39 (m, 5H).

***trans*-8-Azido-*N*-benzyl-4-cycloocten-1-amine (12).** A solution of **11** (10 g, 0.047 mol), sodium azide (12.2 g, 0.19 mol), and ammonium chloride (10.02 g, 0.19 mol) in ethanol (500 mL) and water (100 mL) was refluxed for 4 h. The ethanol was evaporated in vacuo, and the aqueous residue was extracted with 3 × 150 mL CH_2Cl_2. The organic layers were collected and dried (Na_2SO_4), and the solvent was evaporated to give **12** which was isolated as an oil by silica gel flash chromatography, eluting with CH_2Cl_2/ethyl acetate 9:1 (10.96 g, yield 91%).

^{1}H NMR ($CDCl_3$): δ 1.60−1.90 (m, 2H); 2.00−2.25 (m, 4H); 2.30−2.60 (m, 2H); 2.75−3.00 (m, 1H); 3.67 (dt, 1H, J = 8.8 Hz); 3.80 (AB syst, 2H, J = 12.82 Hz); 5.60 (dq, 2H, J = 5.5); 7.10−7.35 (m, 5H).

2-Azido-9-benzyl-5-bromo-9-azabicyclo[4.2.1]nonane (14a), 2-Azido-9-benzyl-6-bromo-9-azabicyclo[3.3.1]nonane (14b). To a solution of **12** (2 g, 7.8 mmol) in cyclohexane (110 mL), stirred at 5 °C in subdued light, was slowly added a solution of 10% bromine in cyclohexane, until a yellow color of the reaction mixture persisted. The solid that separated was filtered (1.6 g), treated with 10% sodium hydroxide, and extracted with ether. The organic layer was dried (Na_2SO_4) and the solvent evaporated. Flash chromatography of the residue on silica gel eluting with petroleum ether 40−60/diethyl ether 98:2 gave in the order **14a** as an oil (0.60 g, yield 23%) and **14b** as a white solid mp 75−76 °C (diethyl ether) (0.50 g, yield 19%).

14a: ^{1}H NMR ($CDCl_3$): δ 1.20−1.60 (m, 2H); 1.70−2.10 (m, 3H); 2.10−2.40 (m, 3H); 3.20−3.40 (m, 1H); 3.56 (q, 1H, J = 4.8 Hz); 3.70−3.90 (m, 3H); 4.12 (t, 1H, J = 7.2 Hz); 7.20−7.45 (m, 5H).

14b: ^{1}H NMR ($CDCl_3$): δ 1.60−2.00 (m, 3H); 2.00−2.50 (m, 5H); 2.90−3.00 (m, 1H); 3.00−3.20 (m, 1H); 3.90−4.20 (m, 3H); 4.30−4.50 (m, 1H); 7.20−7.45 (m, 5H).

The structure of **14b** was supported by X-ray analysis.

9-Benzyl-9,10-diazatricyclo[4.2.1.1^{2,5}]decane 15. To a stirred solution of **14a** (0.4 g, 0.0012 mol) in anhydrous THF (15 mL) at room temperature was added an equimolar amount of triphenylphosphine (0.31 g) in THF (5 mL), and the mixture refluxed for 4 h. After cooling to 0 °C, water (0.1 mL) was added and the mixture was refluxed for additional 15 h. Solvent was removed by coevaporation with ethanol, diethyl ether was added, and the resulting solid was separated and triturated with Et_2O to give **15** as the hydrobromide (0.32 g, 85% yield), mp = 255 °C (MeOH/EtOH).

15: (as free base) mp = 75−76 °C.

^{1}H NMR ($CDCl_3$): δ 1.40−1.60 (m, 2H); 1.70−1.90 (m, 4H); 2.00−2.20 (m, 2H); 2.70−2.90 (m, 2H); 3.00−3.20 (m, 2H); 3.50 (s, 2H); 7.10−7.50 (m, 5H).

The structure of **15** was supported by X-ray analysis.

2-Benzyl-2,7-diazatricyclo[4.4.0.0^{3,8}]decane 18. To a stirred solution of **14b** (1.03 g, 0.0031 mol) in anhydrous THF (30 mL) at room temperature was added an equimolar amount of triphenylphosphine (0.81 g) in THF, and the mixture refluxed overnight. After cooling to 0 °C, water (0.1 mL) was added and the mixture refluxed for an additional 24 h. The reaction was quenched as described for **15.** Flash chromatography of the crude hydrobromide eluting with diethyl ether/6 M NH_3 in MeOH 95:7 gave **18** as free base (0.40 g, yield 56%) mp = 127−128 °C.

^{1}H NMR ($CDCl_3$): δ 1.50−2.30 (m, 8H); 2.60−2.80 (m, 2H); 3.00−3.20 (m, 2H); 3.90 (AB syst, 2H, J = 13.7 Hz); 7.10−7.50 (m, 5H).

9,10-Diazatricyclo[4.2.1.1^{2,5}]decane 4,2,7-Diazatricyclo-[4.4.0.0^{3,8}]decane 5. The appropriate benzyl derivative (**15, 18**) (0.14 g, 0.57 mmol) was dissolved in ethanol (6 mL). To this solution was added 10% Pd/C together with few drops of 6 N hydrochloric acid. The mixture was hydrogenated at room temperature overnight, and the catalyst was filtered off and washed with hot 50% aqueous ethanol. The filtrate was evaporated in vacuo to give **4** and **5** as the dihydrochlorides in quantitative yields (0.078 mg).

4·2HCl: mp = 295 °C dec (EtOH/H_2O/Et_2O).

^{1}H NMR (DMSO): δ 2.00−2.20 (m, 4H); 2.20−2.40 (m, 4H); 3.94 (app. s, 4H); 8.80 (bs, D_2O exchang., 2H).

5.2HCl: mp = 300 °C dec (EtOH/H_2O/Et_2O).

^{1}H NMR (D_2O): δ 1.90−2.20 (m, 4H); 2.20−2.50 (m, 4H); 4.04 (app. d, 4H).

The structure of **5** was supported by X-ray analysis.

9-Propionyl-10-benzyl-9,10-diazatricyclo[4.2.1.1^{2,5}]-decane 16, 2-Propionyl-7-benzyl-2,7-diazatricyclo[4.4.0.0^{3,8}]-decane 19. A solution of propionic anhydride (6.9 mmol) in CH_2Cl_2 (2 mL) was added in one portion to an ice-cooled solution of the appropriate benzyl derivative (**15, 18**) (0.45 g, 1.9 mmol) in CH_2Cl_2 (15 mL). The mixture was refluxed for 1 h, allowed to cool to room temperature, made alkaline with

Table 3. Physicochemical Properties of Compounds **6** and **7**

compd	Ar	mp (°C)	yield (%)	^{1}H NMR
6a	C_6H_5	191−192[b]	95	**(CDCl$_3$):**[a] δ 1.15 (t, 3H, J = 7.6); 1.30−2.20 (m, 8H); 2.28 (q, 2H, J = 7.6); 1.97−3.04 (m, 4H); 3.86 (bs, 1H); 4.49 (bs, 1H); 6.15−6.30 (m, 1H); 6,48 (d, 1H, J = 16.04); 7.20−7.40 (m, 5H)
6b	p-NO_2-C_6H_5	132−133[a]	80	**(CDCl$_3$):**[a] δ 1.19 (t, 3H, J = 7.6); 1.30−2.20 (m, 8H); 2.32 (q, 2H, J = 7.6); 3.06 (m, 4H); 3.92 (bs, 1H); 4.54 (bs, 1H); 6.35−6.55 (m, 1H); 6.63 (d, 1H, J = 16.06); 7.53 (d, 2H, J = 8.9); 8.21 (d, 2H, J = 8.9)
6c	m-NO_2-C_6H_5	237−238[b]	72	**(DMSO):**[b] δ 1.03 (t, 3H, J = 7.4); 1.60−2.20 (m, 6H); 2.30−2.50 (m, 2H); 3.70−4.20 (m, 4H); 4.40−4.60 (m, 2H); 6.70−7.00 (m, 1H); 7.10 (d, 1H, J = 16.0); 7.73 (t, 1H, J = 8); 7.95 (d, 1H, J = 8.0); 8.21(d, 1H, J = 8.0); 8.33 (s, 1H); 10.48 (bs, D_2O exchang., 1H)
6d	m-Cl-C_6H_5	90[b]	85	**(CDCl$_3$):**[a] δ 1.14 (t, 3H, J = 7.5); 1.40−1.80 (m, 6H); 2.00−2.20 (m, 3H); 2.27 (q, 2H J = 7.6); 2.90−3.05 (m, 4H); 3.86 (bs, 1H); 6.10−6.30 (m, 1H); 4.48 (bs, 1H); 6.44 (d, 1H, J = 16.0); 7.18−7.30 (m, 3H); 7.35 (s, 1H)
6e	1-naphthyl	138−142[b]	37	**(CDCl$_3$):**[a] δ 1.17 (t, 3H, J = 7.5); 1.40−2.20 (m, 8H); 2.30(q, 2H, J = 7.6); 3.00 (m, 4H); 3.89 (bs, 1H); 3.20−4.53 (bs, 1H); 6.10−6.40 (m, 1H); 7.20 (d, 1H, J = 16.0); 7.35−7.65 (m, 4H); 7.75−7.90 (m, 2H); 8.00−8.20 (m, 1H)
7a	C_6H_5	220−221[b]	87	**(CDCl$_3$):**[a] δ 1.00−1.60 (m, 5H); 1.60−2.10 (m, 6H); 2.25 (dq, 2H, J = 7.5); 3.00−3.10 (m, 2H); 3.40−3.60 (m, 2H); 3.77 (bs, 1H); 4.31 (bs, 1H); 6.08−6.30 (m, 1H); 6.55 (d, 1H, J = 16.0); 7.42 (m, 5H)
7b	p-NO_2-C_6H_5	135[b]	70	**(DMSO):**[a] δ 1.10 (t, 3H, J = 7.6); 1.40−2.50 (m, 8H); 3.30−3.50 (m, 2H); 3.70−4.50 (m, 4H); 6.80−7.00 (m, 1H); 7.15 (d, 1H, J = 16.06); 7.75 (d, 2H, J = 8.9); 8.28 (d, 2H, J = 8.9)
7c	m-NO_2-C_6H_5	135−137[b]	90	**(CDCl$_3$):**[a] δ 1.16 (t, 3H, J = 7.4); 1.20−1.50 (m, 3H); 1.60−2.10 (m, 5H); 2.10−2.40 (m, 2H); 3.00−3.20 (m, 2H); 3.40−3.70 (m, 2H); 3.80 (bs, 1H); 4.15 (bs, 1H); 6.40−6.70 (m, 1H); 6.20 (d, 1H, J = 16.0); 7.45 (t, 1H, J = 8); 7.65 (d, 1H, J = 8.0); 8.05 (d, 1H, J = 8.0); 8.21 (s, 1H)
7d	m-Cl-C_6H_5	110[b]	65	**(CDCl$_3$):**[a] δ 1.16 (t, 3H, J = 7.5); 1.20−2.10 (m, 8H); 2.26 (dq, 2H, J = 7.6); 2.90−3.10 (m, 2H); 3.40−3.60 (m, 2H); 3.78 (bs, 1H,); 4.30 (bs, 1H); 6.10−6.30 (m, 1H); 6.50 (d, 1H, J = 16.0); 7.18−7.30 (m, 3H); 7.35 (s, 1H)

[a] Free base. [b] Hydrochloride.

excess 40% sodium hydroxide, and stirred overnight. The insoluble was extracted with CH_2Cl_2, the solvent was evaporated, and the oily residue was purified by flash chromatography eluting with petroleum ether 40−60/ethyl acetate 6:4 collecting **16** (0.46 g, 86%) or **19** (0.51 g, 95%) as yellow oils.

16: ^{1}H NMR ($CDCl_3$): 1.14 (t, 3H, J = 7.5 Hz); 1.40−2.22 (m, 8H); 2.27 (q, 2H, J = 7.5 Hz); 2.90−3.05 (m, 2H); 3.84 (app. s, 1H); 3.40 (s, 2H); 4.46 (app. s, 1H); 7.20−7.40 (m, 5H).

19: ^{1}H NMR ($CDCl_3$): δ 1.16 (t, 3H, J = 7.6 Hz); 1.10−2.10 (m, 8H); 2.27 (q, 2H, J = 7.7 Hz); 2.90−3.00 (m, 2H); 3.70−3.80 (m, 1H); 3.92 (AB syst, 2H, J = 13.9 Hz); 4.30−4.35 (m, 1H); 7.10−7.40 (m, 5H).

9-Propionyl-9,10-diazatricyclo[4.2.1.1^{2,5}]decane 17, 2-Propionyl-2,7-diazatricyclo[4.4.0.0^{3,8}]decane 20. The appropriate benzyl derivative (**16, 19**) was hydrogenated as described for **4** and **5**, affording **17** and **20** as the hydrochlorides (yield 96%).

17·HCl: mp = 230 °C.

^{1}H NMR (free base) ($CDCl_3$): δ 1.11 (t, 3H, J = 7.5 Hz); 1.21−2.10 (m, 8H); 2.24 (q, 2H, J = 7.6 Hz); 3.13−3.25 (m, 2H); 3.79−3.87 (m, 1H); 4.45−4.47 (m, 1H).

20·HCl: mp = 234 °C.

^{1}H NMR ($CDCl_3$): δ 1.19 (t, 3H, J = 7.5 Hz); 1.49−1.79 (m, 2H); 1.80−2.50 (m, 8H); 3.78−4.00 (m, 3H); 4.40−4.50 (m, 1H).

9-Propionyl-10-arylalkenyl-9,10-diazatricyclo[4.2.1.12,5]-decane (6a−e), 2-Propionyl-7-arylalkenyl-2,7-diazatricyclo-[4.4.0.03,8]decane (7a−d). A mixture of the appropriate propionyl derivative (**17**, **20**) (1.1 mmol), the appropriate arylalkenyl chloride (1.1 mmol), and K_2CO_3 (1.1 mmol) in acetone was refluxed for 24 h. The inorganic salts were filtered off, the filtrate was evaporated, and the residue was purified by silica gel flash chromatography, eluting with petroleum ether 40−60/ethyl acetate to give **6** and **7**. (See Table 3 for the physicochemical properties of **6** and **7**.)

Pharmacology. Binding. Rat and guinea-pig brain membrane binding studies were carried out as described by Gillan and Kosterlitz[8] with slight modifications. Briefly, membranes were freshly prepared from whole brains minus cerebellum. ^{3}H-DAMGO (1 nM) and DELTORPHINE II (1 nM) were used to label μ- and δ-receptors. U69593 (1 nM) was used to label κ-receptors in guinea pig brain membranes. Membranes were incubated with the appropriate ^{3}H-ligand in 50 mM Tris HCl pH 7.4 at 25 °C for 60 min in the absence or in the presence of 10 μM BREMAZOCINE. Final protein concentration was determined by the method of Lowry et al., with bovine serum albumin as standard.[9]

Antinociception. Male Albino-Swiss mice weighing 20−25 g (Charles River Italy) were used. Antinociception was estimated by means of the hot plate method described by Oden and Oden.[10] The effect of compounds on the reaction time of mice placed on a hot plate thermostatically maintained at 56 °C was determined. The time at which mice displayed a nociceptive response, i.e., licking the front paws, fanning the hind paws, or jumping, was recorded. The 50% antinociceptive doses (ED_{50}) and their 95% confidence intervals were determined by the method of Litchfield and Wilcoxon.[11] The antagonistic effect of naloxone on **6a** and **7a** induced antinociception was measured by administering naloxone (1 mg/kg) or vehicle ip at time 0.

Molecular Modeling. All molecular modeling was performed with use of the software package SYBYL[10] running on a Silicon Graphics R10000 workstation. Herein we describe the computational procedure applied to the diazatricyclodecane derivatives **6a** and **7a**.

Molecular models of compounds **6a** and **7a** (in Chart 3) were constructed using standard bond lengths and bond angles of the SYBYL fragment library. Ligands were modeled in their nitrogen-protonated form. The October 1996 and April 1977 releases (3D graphics 5.12 and 5.13 versions for Unix platforms) of the CSD[24] were searched through substructure queries using the CSD/QUEST graphical routine. Conformational energies were calculated employing the molecular mechanics TRIPOS force field[25] with neglect of electrostatics. Energy minimizations were realized with the SYBYL/MAXIMIN2 option by applying the BFGS (Broyden, Fletcher, Goldfarb, and Shannon) algorithm[26] and setting a root-mean-square gradient of the forces acting on each atom of 0.05 kcal/mol Å as the gradient convergence criterion.

The conformation of the *N*-cinnamyl substituent is primarily determined by the torsion angles τ_2 and τ_3, as depicted in Figure 9. Owing to π-conjugation, the τ_4 value can be either 0° or 180°.[27]

A conformational analysis was preliminary performed on the 2*R*,3*R*,5*S*,6*S* enantiomer of **6a** and 2*S*,3*S*,5*S*,6*S* enantiomer of **7a** by varying τ_2 and τ_3 torsions in the RANDOM-SEARCH option[28] of the SYBYL program. In this Monte Carlo-like method, many conformations are generated by randomly perturbing selected rotatable bonds and then energy-mini-

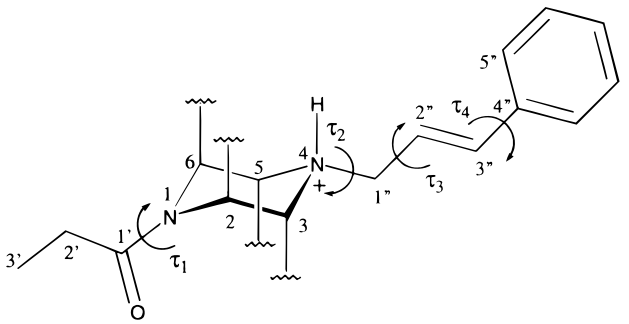

Figure 9. Definition of the torsion angles τ_1 (C2′-C1′-N1-C2), τ_2 (H_{N4}-N4-C1″-C2″), which primarily determines the direction of the N-substituent, τ_3 (N4-C1″-C2″-C3″), and τ_4 (C2″-C3″-C4″-C5″).

Table 4. Main Torsion Angles[a] (deg) and Strain Energies of Compounds (2*R*,3*R*,5*S*,6*S*)-**6a** and (2*S*,3*S*,5*S*,6*S*)-**7a** Resulting from Conformational Analysis

compd	conformation	τ_1	τ_2	τ_3	τ_4	ΔE_{conf}[b]
6a	1	169	−59	95	22	0.0
	2	169	52	−102	154	0.1
7a	1′	−179	55	110	156	0.0
	2′	−180	−59	101	156	0.2

[a] The torsion angles are defined as follows on the basis of the atom numbering scheme reported in Figure 1. [b] ΔE_{conf} is the strain energy calculated with TRIPOS force field as the difference in energy between the conformation and the global minimum conformer.

mized. Each new conformation is compared against all others found so far to see if it is unique. RANDOMSEARCH was run under the following settings (reported in parentheses): (a) the maximum number of hits, which defines the number of times each conformation must be found to stop the search for new conformations (n = 6); (b) the root-mean-squares (RMS) threshold, which defines the maximum RMS difference between two conformations before they are considered different (1 Å for **6a** and 0.7 Å for **7a**); (c) the energy cutoff, which defines the maximum allowed energy for a conformation to be kept and energy-minimized (E = energy of the input conformer plus 50 kcal/mol); (d) the maximum number of attempts to find a new conformation (1000 for both compounds). Since τ_1, associated to the rotation of the amide bond, can be either 0° or 180°, this torsion was not scanned in the conformational analysis, but arbitrarily fixed to 180°. Energies were computed through the molecular mechanics TRIPOS force field.[25]

Among the resulting conformations, only those associated with energy within 3 kcal/mol from the global minimum (two for **6a** and two for **7a**) were further evaluated for their ability to fit the μ-opioid receptor model[8] by docking studies. Table 4 summarizes the most relevant torsional angles defining the low-energy conformations of **6a** and **7a**.

Docking. The μ-opioid receptor model used for docking calculations was that developed by Pogozheva et al.[8] A detailed description of the model, including the coordinates, is available on the Internet at http://www-personal.umich.edu.

A number of site-directed mutagenesis studies have been performed on the μ-opioid receptors.[11,12,16] The following conclusions can be drawn: (i) the carboxylate group of Asp147 in transmembrane domain III (TM3) has been demonstrated to interact with the positively charged nitrogen found in many opioid ligands; (ii) the phenolic hydroxyl group of various opiates is postulated to form a hydrogen bond with the His297 imidazole ring, which is located in the sixth transmembrane spanning helix (TMVI).

We manually docked into the helical bundle both conformations 1 and 2 of 2*R*,3*R*,5*S*,6*S*-**6a** (see Table 4) in such a way that the ammonium nitrogen was placed near the aspartate carboxylate group on TMIII and the carbonyl oxygen of the acyl chain was in the proximity of the His297 imidazole ring. Only the conformation 1 fitted well into the receptor model, according to restraints discussed above. During the docking maneuvre, we tried both 0° and 180° arragements for τ_1, the latter result being more favorable owing to the possibility for the propionyl oxygen to accept a hydrogen bond from the His297 side chain. The docked structure of conformation 1 was used as a template to align the conformations 1′ and 2′ of 2*S*,3*S*,5*S*,6*S*-**7a** (see Table 4). These structures were superimposed on the docked compound **6a** by fitting the carbonyl group, the ammonium nitrogen, and its proton. Conformation 1′ could not be accommodated in the μ-opioid receptor model, as the styrene portion of its N-substituent caused severe steric hindrance with the side chain Ile144 in helix III. In contrast, conformation 2′ was completely superimposable on **6a**, occupying a similar binding region at the μ-receptor model. Conformation 1 of 2*R*,3*R*,5*S*,6*S*-**6a** and conformation 2′ of 2*S*,3*S*,5*S*,6*S*-**7a** were then converted into their mirror images using the SYBYL/INVERT option, thus obtaining the corresponding isoenergetic 2*S*,3*S*,5*R*,6*R* and 2*R*,3*R*,5*R*,6*R* conformers, differing only in the sign of the torsional angles. These two enantiomers were each in turn placed into the μ-opioid binding site, by fitting them on the corresponding docked enantiomer.

Molecular dynamics (MD) simulations were performed using the AMBER 4.1 suite of programs[29] based on the Cornell et al. force field.[30] Partial atomic charges for the ligands were calculated with the semiempirical quantum-mechanics method AM1,[31] available in the MOPAC program,[32] and imported from the output files. The resulting receptor−ligand complexes were energy-mimimized in vacuo with the SANDER module of AMBER 4.1 (50 000 steps; distance dependent dielectric function of $\epsilon = 4r$), applying an energy penalty force constant of 5 kcal/mol on the protein backbone atoms. The geometry-optimized structures were then used as the starting point for subsequent 200 ps MD simulation, during which the protein backbone atoms were constrained as done in previous step. A 1 fs time step was used along with a nonbonded pairlist updated every 25 fs. The temperature was mantained at 300 K using Beredensen algorithm[33] with a 0.2 ps coupling constant.

For each of the four complexes, an average structure was calculated from the last 100 ps trajectory and energy-minimized using the steepest descent and conjugate gradient methods available within the SANDER module of AMBER 4.1 as specified above. The resulting models were then subsequently analyzed by evaluating the ligand−protein interaction energy (steric plus electrostatic).

Supporting Information Available: Elemental analysis for compounds **4**−**7**, **12**, and **14**−**20** (Table 5); crystal data; experimental and refinements details; tables of coordinates; temperature factors; bond distances and angles for compounds **5**, **14b**, and **15** (Tables 6−23). This material is available free of charge via the Internet at http://pubs.acs.org.

References

(1) (a) Cignarella, G.; Nathansohn, G. G. Bicyclic Homologues of Piperazine. II. Synthesis of 3,8-diazabicyclo[3.2.1]octane. *J. Org. Chem.* **1961**, *26*, 2747−2750. (b) Cignarella, G.; Testa, E.; Pasqualucci, C. R. Thermal and Chemical Intramolecular Migration in 8-acyl-3,8-diazabicyclo[3.2.1]octanes. *Tetrahedron* **1963**, *19*, 143−148.

(2) Cignarella, G.; Occelli, E.; Testa, E. Bicyclic Homologues of Piperazine. VII. Synthesis and Analgesic Activity of 3-aralkenyl-8-propionyl-3,8-diazabicyclo[3.2.1]octanes *J. Med. Chem.* **1965**, *8*, 326−331.

(3) Cignarella, G.; Barlocco, D.; Tranquillini, M. E.; Volterra, A.; Brunello, N.; Racagni, G. Interaction of 3,8-diazabicyclo[3.2.1]-octanes with μ and δ Opioid Receptors. *Pharm. Res. Commun.* **1988**, *20*, 383−393.

(4) Fadda, P.; Barlocco, D.; Tronci, S.; Cignarella, G.; Fratta, W. Antinociceptive Action of DBO 17 and DBO 11 in Mice: Two 3,8-Diazabicyclo[3.2.1]octane Derivatives with Selective μ Opioid Receptor Affinity. *Naunyn-Schmeideberg's Arch. Pharmacol.* **1997**, *356*, 596−602.

(5) Barlocco, D.; Cignarella, G.; Greco, G.; Novellino, E. Computer-Aided Structure-Affinity Relationships in a Set of Piperazine and 3,8-Diazabicyclo[3.2.1]octane Derivatives Bindig to the μ Opioid Receptor. *J. Comput.-Aided Mol. Des.*, **1993**, *7*, 557−571.

(6) Crandall, J. K.; Banks, D. B.; Colyer, R. A.; Watkins, R. J.; Arrington, J. P. A Synthesis of Homoallylic Alcohols. *J. Org. Chem.* **1968**, *33* (1), 423−425.
(7) Chini, M.; Crotti, P.; Favero, L.; Macchia, F.; Pineschi, M. Lanthanide (III) Trifluoromethanesulfonates as Extraordinarily Effective New Catalysts for the Aminolysis of 1,2-epoxides. *Tetrahedron Lett.* **1994**, *35* (3), 433−436.
(8) Pogozheva, I. D.; Lomize, A. L.; Mosberg, H. I. Opioid Receptor Three-Dimensional Structures from Distance Geometry Calculations with Hydrogen Bonding Constraints. *Biophys. J.* **1998**, *75*, 612−634.
(9) Pogozheva, I. D.; Lomize, A. L.; Mosberg, H. I. The Transmembrane 7-α-Bundle of Rhodopsin: Distance Geometry Calculation with Hydrogen Bonding Constraints. *Biophys. J.* **1997**, *70*, 1963−1985.
(10) Sybyl Molecular Modelling System (version 6.2), Tripos Ass., St. Louis, MO.
(11) Surratt, C. K.; Johnson, P. S.; Moriwaki, A.; Seidleck, B. K.; Blaschak, C. J.; Wang, J. B.; Uhl, G. R. μ-Opioid Receptor. Charged Transmembrane Domain Amino Acids are Critical for Agonist Recognition and Intrinsic Activity. *J. Biol. Chem.* **1994**, *269*, 20548−20553.
(12) Heerding, J.; Raynor, K.; Kong, H.; Yu, L.; Reisine, T. Mutagenesis Reveals that Agonists and Peptide Antagonists Bind in Fundamentally Distinct Manners to the Rat Mu Receptor than Do Nonpeptide Antagonists. *Regul. Pept.* **1994**, *54*, 119−120.
(13) Hibert, M. F.; Trumpp-Kallmeyer, S.; Bruinvels, A.; Hoflack, J. Three-Dimensional Models of Neurotransmittes G-Binding Protein-Coupled Receptors. *Mol. Pharmacol.* **1991**, *40*, 8−15.
(14) Trumpp-Kallmeyer, S.; Hoflack, J.; Bruinvels, A.; Hibert, M. F. Modeling of G-Protein-Coupled Receptors: Application to Dopamine, Adrenaline, Serotonin, Acetylcholine, and Mammalian Opsin Receptors. *J. Med. Chem.* **1992**, *35*, 3448−3462.
(15) Verdonk, M. L.; Boks, G. J.; Kooijman, H.; Kanters, J. A.; Kroon, J. *J. Comput.-Aided Mol. Des.* **1993**, *7*, 173−182.
(16) Mansour, A.; Taylor, L. P.; Fine, J. L.; Thompson, R. C.; Hoversten, M. T.; Mosberg, H. I.; Watson, S. J.; Akil, H. Key Residues Defining the μ-Opioid Receptor Binding Pocket: A Site-Directed Mutagenesis Study. *J. Neurochem.* **1997**, *68*, 344−353.
(17) Barlocco, D.; Cignarella, G.; Vianello, P.; Villa, S.; Pinna, G. A.; Fadda, P.; Fratta, W. Synthesis and μ-Opioid Receptor Affinity of a New Series of Nitro Substituted 3,8-Diazabicyclo[3.2.1]-octane Derivatives. *Il Farmaco* **1998**, *53*, 557−562.
(18) Xu, H.; Lu, Y. F.; Partilla, J. S.; Zheng, Q. X.; Wang, J. B.; Brine, G. A.; Carroll, F. I.; Rice, K. C.; Chen, K. X.; Chi, Z. Q.; Rothman, R. B. Opioid Peptide Receptor Studies, 11: Involvement of Tyr148, Trp318 and His319 of the Rat Mu-Opioid Receptor in Binding of Mu-Selective Ligands. *Synapse* **1999**, *32*, 23−28.
(19) Burley, S. K.; Petsko, G. A. Aromatic−Aromatic Interaction: a Mechanism of Protein Structure Stabilitation. *Science* **1995**, *229*, 23−28.
(20) Gillan, M. G. C.; Kosterlitz, H. W. Spectrum of μ, δ, and κ Binding Sites in Homogenates of Rat Brain. *Br. J. Pharmacol.* **1982**, *77*, 461−469.
(21) Lowry, O. H.; Rosebrough, N. J.; Farr, A. L.; Randall, R. J. Protein Measurement with Folin Phenol Reagent. *J. Biol. Chem.* **1951**, *193*, 265−275.
(22) Oden, D. L.; Oden, K. L. A Minimum Stress Procedure for Repeated Measurement of Nociceptive Threshold Analgesia. *Life Sci.* **1982**, *31*, 1245−1248.
(23) Litchfield, J. T.; Wilcoxon, F. A Simplified Method of Evaluating Dose Effect Experiment. *J. Pharmacol. Exp. Ther.* **1949**, *96*, 99−113.
(24) Allen, F. H.; Bellard, S.; Brice, M. D.; Cartwright, B. A.; Doubleday, A.; Higgs, H.; Hummelink, T.; Hummelink-Peters, B. G.; Kennard, O.; Motherwell, W. D. S.; Rodgers, J. R.; Watson, D. G. The Cambridge Crystallographic Data Centre: Computer-Based Search, Retrieval, Analysis and Display of Information. *Acta Crystallogr.* **1979**, *B35*, 2331−2339.
(25) Vinter, J. G.; Davis, A.; Saunders: M. R. Strategic Approaches to Drug Design. 1. An Integrated Software Framework for Molecular Modelling. *J. Comput.-Aided Mol. Des.* **1987**, *1*, 31−55.
(26) Head, J.; Zerner, M. C. A Broyden-Fletcher-Goldfarb-Shanno Optimization Procedure for Molecular Geometries. *Chem. Phys. Lett.* **1985**, *122*, 264−274.
(27) This conformational preference was confirmed by a substructure search in the Cambridge Structural Database (CSD).[26] Using CCCH═CHAr as a query, we identified 213 hits characterized by an absolute value of the torsion angle τ_4 falling in the ranges 0°−20° and 160°−180°, all implying an orientation of the aromatic ring out of the plane of the double bond.
(28) Treasurywala, A. M.; Jaeger, E. P.; Peterson, M. L. Conformational Searching Methods for Small Molecules. III. Study of Stochastic Methods Available in SYBYL and MACROMODEL. *J. Comput. Chem.* **1996**, *17*, 1171−1182.
(29) (a) Pearlman, D. A.; Case, D. A.; Caldwell, J. W.; Ross, W. S.; Cheatham, T. E., III; Debolt, S.; Ferguson, D. M.; Seibel, G. L.; Kollman, P. A. AMBER, a Package of Computer Programs for Applying Molecular Mechanics, Normal-Mode Analysis, Molecular Dynamics and Free Energy Calculations to Simulate the Structural and Energetic Properties of Molecules. *Comput. Phys. Commun.* **1995**, *91*, 1−41. (b) Pearlman, D. A.; Case, D. A.; Caldwell, J. W.; Ross, W. S.; Cheatham, T. E., III; Ferguson, D. M.; Seibel, G.; Singh, U. C.; Weiner, P. K.; Kollman, P. A. AMBER 4.1, Department of Pharmaceutical Chemistry, University of California, San Francisco, CA, 1995.
(30) Cornell, W. D.; Cieplak, P.; Bayly, C. I.; Gould, I. R.; Merz, K. M.; Ferguson, D. M.; Spellmeyer, D. C.; Fox, T.; Caldwell, J. W.; Kollman, P. A. A Second Generation Force Field for the Simulation of Proteins, Nucleic Acids, and Organic Molecules. *J. Am. Chem. Soc.* **1995**, *117*, 5179−5197.
(31) Dewar, M. J. S.; Zoebisch, E. G.; Healy, E. F.; Stewart, J. J. P. AM1: a New General Purpose Mechanical Molecular Model. *J. Am. Chem. Soc.* **1985**, *107*, 3902−3909.
(32) MOPAC (version 6.0) is available from Quantum Chemistry Program Exchange, No. 455.
(33) Berendsen, H. J. C.; Postma, J. P. M.; van Gunsteren, W. F.; DiNola, A.; Haak, J. R. Molecular Dynamics with Coupling to an External Bath. *J. Chem. Phys.* **1984**, *81*, 3684−3690.

JM991140Q